Bounded, Periodic Relative Motion using Canonical Epicyclic Orbital Elements

N. Jeremy Kasdin* **& Egemen Kolemen†**
Princeton University

ABSTRACT

In this paper, we use a Hamiltonian approach to derive the equations of motion for an object relative to a circular or slightly elliptical reference orbit. By solving the Hamilton-Jacobi equation we develop constants of the relative motion called epicyclic elements. A perturbation Hamiltonian is formulated in order to derive variational equations for the "constants" via Hamilton's equations. We use this formalism to derive bounded, periodic orbits in the presence of various perturbations. In particular, we show a simple no-drift condition that guarantees bounded orbits in the presence of J_2 forces. We also derive the relative motion deviations and boundedness conditions due to eccentricity of the reference orbit and higher-order terms in the gravitational potential.

1. INTRODUCTION

This paper presents a new approach to modeling the motion of objects relative to a circular or elliptic reference orbit and for finding bounded trajectories in the presence of perturbations. The problem of bounded relative motion is becoming of increasing interest as future missions begin to rely on multiple spacecraft in formation for carrying out their objectives. The most prominent among these are the formation flying interferometers. For example, NASA expects to fly its second Terrestrial Planet Finder mission, TPF-I, in 2019. This will consist of at least three satellites forming a nulling interferometer to image extrasolar earthlike planets in the infra-red. While control will certainly be needed to maintain the closed formations necessary for these missions, it is still extremely beneficial to develop accurate models and bounded solutions to minimize the use of fuel. In this paper, we present a novel approach using canonical perturbation theory for studying relative motion trajectories and for finding simple conditions for periodic orbits.

Traditional approaches to relative motion have relied upon the second-order Clohessy-Wiltshire (CW) equations to describe small deviations from a circular reference orbit [1]. These can easily be solved and use the relative initial conditions as constants of the motion. Unfortunately, this is often an inconvenient and difficult method for treating perturbations to the relative motion. Alternatively, many researchers have turned to an orbital elements or inertial description of the relative motion [2, 3, 4, 5]. This has the advantage that Lagrange's planetary equations (LPEs) or Gauss's variational equations (GVEs) can be used to treat small perturbations; nevertheless, orbital elements are an indirect representation of relative motion and the beauty and convenience of treating the motion entirely in a Hill frame is lost.

In [6] we describe a new approach to treating relative motion that unifies these treatments. We describe the motion in the rotating Hill frame via a low-order Hamiltonian and solve the Hamilton-Jacobi equation. This results in a first-order solution to the relative motion identical to the usual CW approach; here, though, rather than using initial conditions as our constants of the motion, we have the canonical momenta and coordinates. This allows us to treat perturbations in an identical manner as in the classical Delaunay formulation of the two-body problem. By treating the perturbations or high-order terms as a perturbing Hamiltonian, we can find variational equations for the new constants via Hamilton's equations. We find that this can greatly simplify the search for boundedness conditions and provides a compact and insightful description of the resulting motion.

*Assistant Professor, Mechanical and Aerospace Engineering, Princeton, NJ 08544, jkasdin@princeton.edu
†Doctoral Student, Mechanical and Aerospace Engineering, Princeton, NJ 08544, ekolemen@princeton.edu

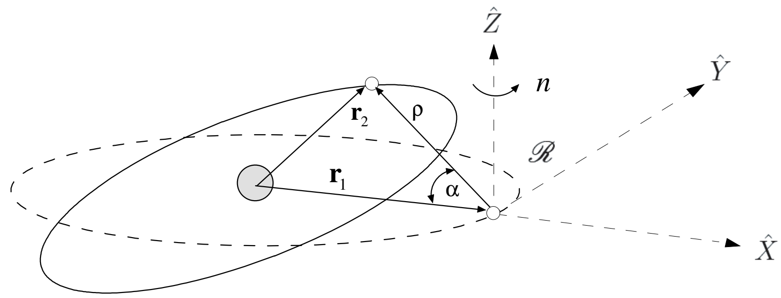

Figure 1. Relative motion rotating Euler-Hill reference frame

In the next section we briefly summarize the development of the H-J solution and variational equations from [6]. We then follow with three perturbation examples. In Section 3 we use the technique to solve for the effect of the the higher terms in the potential expansion and derive the boundedness condition including second- and third-order terms. In Section 4 we summarize our results from [6] for the $J2$ perturbation on a satellite formation. Finally, in Section 5 we use the same approach to find the first-order variations due to a small eccentricity of the reference orbit. We then show how these can be combined to formulate the net relative motion.

2. THE HAMILTON-JACOBI SOLUTION OF RELATIVE MOTION

For this study, we are considering the motion of a satellite in a Cartesian Euler-Hill frame relative to a circular orbit as shown in Figure 1. Motion relative to orbits of small eccentricity will be treated via perturbations in powers of e in Section 5. Traditionally, relative motion in this frame has been modeled using the Clohessy-Wiltshire (CW) equations via a first-order, linear analysis:

$$\ddot{x} - 2n\dot{y} - 3n^2 x = Q_x \qquad (1)$$

$$\ddot{y} + 2n\dot{x} = Q_y \qquad (2)$$

$$\ddot{z} + n^2 z = Q_z \qquad (3)$$

where (Q_x, Q_y, Q_z) represent small perturbing forces and n is the reference orbit rate.

In the absence of perturbing forces, it is well known that the solution to these equations consists of an elliptical trajectory about the origin with a possible long term drift. The drift can be eliminated by the no-drift constraint, $\dot{y} + 2nx = 0$.

In this work, we approach the problem slightly differently by first formulating the Lagrangian of the motion in the rotating frame (where we have expanded the potential in terms of Legendre polynomials),

$$\begin{aligned} \mathcal{L} &= \frac{1}{2}\left\{(\dot{x} - ny)^2 + (\dot{y} + nx + na)^2 + \dot{z}^2\right\} \\ &\quad + n^2 a^2 \sum_{k=0}^{\infty} P_k(\cos\alpha)\left(\frac{\rho}{a}\right)^k - U_p \end{aligned} \qquad (4)$$

and U_p is a perturbing potential. Our goal is to formulate a Hamiltonian for the entire system, $\mathcal{H} : \mathbb{R}^3 \times \mathbb{R}^3 \to \mathbb{R}^1$, that we can partition into a nominal Hamiltonian, $\mathcal{H}^{(0)}$, with which we can solve the Hamilton-Jacobi (H-J) equation, and a perturbing Hamiltonian, $\mathcal{H}^{(1)}$,

$$\mathcal{H} = \mathcal{H}^{(0)} + \mathcal{H}^{(1)} \qquad (5)$$

By solving the H-J equation on $\mathcal{H}^{(0)}$, we find a set of canonical momenta and coordinates for which $\mathcal{H}^{(0)}$ is a constant. Thus, perturbations can be treated as causing first-order variations of these new coordinates via Hamilton's equations on the perturbing Hamiltonian. This same procedure is followed in the two-body problem to derive Delaunay variables and the corresponding variational equations.

The first step is to drop the perturbing potentials (which include the higher-order terms in the nominal potential), just as in the treatment leading to the Clohessy-Wiltshire equations for relative motion. This is equivalent to only examining small deviations from the reference orbit. We do this by expanding the potential term to second-order to find the low order Lagrangian,

$$\bar{\mathcal{L}}^{(0)} = \frac{1}{2}\left(\dot{x}^2 + \dot{y}^2 + \dot{z}^2\right) + ((x+1)\dot{y} - y\dot{x}) + \frac{3}{2} + \frac{3}{2}x^2 - \frac{1}{2}z^2 \tag{6}$$

Where we have also normalized rates by n so that time is in units of radians, or the argument of latitude, and we have normalized distances by the reference orbit semi-major axis, a. Not surprisingly, applying the Euler-Lagrange equations to this Lagrangian results in the expected C-W equations, Eqs. (1) - (3).

For brevity, we do not repeat the entire H-J solution procedure here. Details can be found in [6]. Using the Lagrangian in Eq. (6) we find the canonical momenta,

$$\begin{aligned} p_x &= \frac{\partial \mathcal{L}^{(0)}}{\partial \dot{x}} = \dot{x} - y \\ p_y &= \frac{\partial \mathcal{L}^{(0)}}{\partial \dot{y}} = \dot{y} + x + 1 \\ p_z &= \frac{\partial \mathcal{L}^{(0)}}{\partial \dot{z}} = \dot{z} \end{aligned} \tag{7}$$

and the corresponding unperturbed Hamiltonian,

$$\mathcal{H}^{(0)} = \frac{1}{2}(p_x + y)^2 + \frac{1}{2}(p_y - x - 1)^2 + \frac{1}{2}p_z^2 - \frac{3}{2} - \frac{3}{2}x^2 + \frac{1}{2}z^2 \tag{8}$$

This Hamiltonian is used to solve the H-J equation, resulting in a new set of canonical momenta, $(\alpha_1, \alpha_2, \alpha_3)$, and canonical coordinates, (Q_1, Q_2, Q_3),

$$\begin{aligned} \alpha_1 &= \frac{1}{2}(p_x + y)^2 + 2(p_y - x - 1)^2 + \frac{9}{2}x^2 + 6x(p_y - x - 1) \\ &= \frac{1}{2}\left(\dot{x}^2 + (2\dot{y} + 3x)^2\right) \end{aligned} \tag{9}$$

$$\alpha_2 = \frac{1}{2}p_z^2 + \frac{1}{2}z^2 = \frac{1}{2}\dot{z}^2 + \frac{1}{2}z^2 \tag{10}$$

$$\alpha_3 = p_y + x - 1 = \dot{y} + 2x \tag{11}$$

$$\begin{aligned} Q_1 &= u - u_0 + \beta_1 = \tan^{-1}\left(\frac{x - 2\alpha_3}{\sqrt{2\alpha_1 - 4\alpha_3^2 + 4\alpha_3 x - x^2}}\right) \\ &= -\tan^{-1}\left(\frac{3x + 2\dot{y}}{\dot{x}}\right) \end{aligned} \tag{12}$$

$$\begin{aligned} Q_2 &= u - u_0 + \beta_2 = \tan^{-1}\left(\frac{z}{\sqrt{2\alpha_2 - z^2}}\right) \\ &= \tan^{-1}\left(\frac{z}{\dot{z}}\right) \end{aligned} \tag{13}$$

$$\begin{aligned} Q_3 &= -3\alpha_3(u - u_0) + \beta_3 = y - 2\sqrt{2\alpha_1 - 4\alpha_3^2 + 4\alpha_3 x - x^2} \\ &= -2\dot{x} + y \end{aligned} \tag{14}$$

where $(\beta_1, \beta_2, \beta_3)$ are constants and the Hamiltonian in the new coordinates is,

$$\mathcal{H}^{(0)} = \alpha_1 + \alpha_2 \tag{15}$$

In the absence of perturbations, these new coordinates are, of course, constant and given by the Cartesian initial conditions via Eqs. (9) - (14). We call them "epicyclic elements" as they describe epicycle-like motion about a reference circular orbit. These equations can then be solved for x, y, and z to yield the cartesian generating solution in the Hill frame,

$$x(t) = 2\alpha_3 + \sqrt{2\alpha_1}\sin(Q_1) = 2\alpha_3 + \sqrt{2\alpha_1}\sin(u - u_0 + \beta_1) \tag{16}$$
$$y(t) = Q_3 + 2\sqrt{2\alpha_1}\cos(Q_1) = -3\alpha_3(u - u_0) + \beta_3 + 2\sqrt{2\alpha_1}\cos(u - u_0 + \beta_1) \tag{17}$$
$$z(t) = \sqrt{2\alpha_2}\sin(Q_2) = \sqrt{2\alpha_2}\sin(u - u_0 + \beta_2) \tag{18}$$

It is also straightforward to find expressions for the cartesian rates and the canonical momenta in terms of these new variables. Eqs. (16) - (17) are the same elliptic motion solution as one gets from the C-W equations, except here written in terms of the new elements rather than Cartesian initial conditions. The value of this approach is in the canonicity of these elements. Because they solve the H-J equation, if we write the perturbing Hamiltonian in terms of them, we find that their variation under perturbations is given by the first-order Hamilton's equations,

$$\dot{\alpha}_i = -\frac{\partial \mathcal{H}^{(1)}}{\partial Q_i} \tag{19}$$
$$\dot{\beta}_i = \frac{\partial \mathcal{H}^{(1)}}{\partial \alpha_i} \tag{20}$$
$$\dot{Q}_i = \frac{\partial \mathcal{H}^{(0)}}{\partial \alpha_i} + \dot{\beta}_i \tag{21}$$

Before proceeding with our treatment of perturbations, there is one more helpful simplification. The epicyclic elements above parameterize the motion in terms of amplitude and phase. Also, as the α's enter in as square roots, the variational equations can become quite complicated (and often singular). It is therefore often more convenient to introduce an alternative, amplitude like set via the canonical transformation,

$$a_1 = \sqrt{2\alpha_1}\cos\beta_1 \tag{22}$$
$$b_1 = \sqrt{2\alpha_1}\sin\beta_1 \tag{23}$$
$$a_2 = \sqrt{2\alpha_2}\cos\beta_2 \tag{24}$$
$$b_2 = \sqrt{2\alpha_2}\sin\beta_2 \tag{25}$$
$$a_3 = \alpha_3 \tag{26}$$
$$b_3 = \beta_3 \tag{27}$$

It can be shown that this set arises from two symplectic transformations from (α_i, Q_i). Thus, the variations of these new variables are also given by Hamilton's equations on the perturbing Hamiltonian. We call these new elements *contact epicyclic elements*. The new Cartesian position equations in terms of the contact elements become,

$$x(t) = 2a_3 + a_1\sin(u - u_0) + b_1\cos(u - u_0) \tag{28}$$
$$y(t) = b_3 - a_3(u - u_0) - 2b_1\sin(u - u_0) + 2a_1\cos(u - u_0) \tag{29}$$
$$z(t) = b_2\cos(u - u_0) + a_2\sin(u - u_0) \tag{30}$$

3. HIGHER-ORDER NONLINEAR PERTURBATIONS

We treat the effect of the neglected higher-order terms in the expanded potential as our first perturbation. A number of researcher have examined these higher-order terms in recent years in the context of the CW equations [7, 8, 9]. In fact, Richardson [9] presents an approximate solution to the Cartesian relative motion up to third-order using a Poincarè-Lindstedt procedure. Here, we use a very similar procedure but on the variations of the epicyclic elements. The first-order variational equations we find are much simpler to solve, present added insight, and are more easily combined with other perturbations. Our final result agrees well with [9], verifying our method.

The variational equations for the epicyclic elements due to the higher-order potential terms are quite straightforward to find. The perturbing Hamiltonian is simply the higher-order Legendre polynomials in the expansion of the potential,

$$\mathcal{H}^{(1)} = x^3 - \frac{3}{2}x(y^2+z^2) - x^4 + 3x^2(y^2+z^2) - \frac{3}{4}y^2z^2 - \frac{3}{8}(y^4+z^4) \tag{31}$$

where we have included here the third and fourth order terms. The variational equations are found by substituting for (x, y, z) from Eqs. (28)-(30) and using Hamilton's equations on the elements. For brevity, we present only the second-order variational equations,

$$\dot{a_1} = \frac{-3}{8}\left(\begin{array}{l} -4q_3^2\cos(u) - 16q_3\cos(2u)a_1 - 2\cos(u){a_1}^2 - 14\cos(3u){a_1}^2 - \cos(u){a_2}^2 \\ +\cos(3u){a_2}^2 + 32q_3\sin(u)a_3 + 48\sin(2u)a_1a_3 + 32\cos(u){a_3}^2 \\ +16q_3\sin(2u)b_1 - 4\sin(u)a_1b_1 + 28\sin(3u)a_1b_1 - 16a_3b_1 + 48\cos(2u)a_3b_1 \\ -6\cos(u){b_1}^2 + 14\cos(3u){b_1}^2 - 2\sin(u)a_2b_2 - 2\sin(3u)a_2b_2 \\ -3\cos(u){b_2}^2 - \cos(3u){b_2}^2 \end{array}\right) \tag{32}$$

$$\dot{a_2} = \frac{3}{4}\left(\begin{array}{l} \cos(u)a_1a_2 - \cos(3u)a_1a_2 + 4\sin(2u)a_2a_3 + \sin(u)a_2b_1 + \sin(3u)a_2b_1 \\ +\sin(u)a_1b_2 + \sin(3u)a_1b_2 + 4a_3b_2 + 4\cos(2u)a_3b_2 + 3\cos(u)b_1b_2 \\ +\cos(3u)b_1b_2 \end{array}\right) \tag{33}$$

$$\dot{a_3} = 3\left(\begin{array}{l} q_3\sin(u)a_1 + \sin(2u){a_1}^2 + 2q_3a_3 + 4\cos(u)a_1a_3 + q_3\cos(u)b_1 \\ +2\cos(2u)a_1b_1 - 4\sin(u)a_3b_1 - \sin(2u){b_1}^2 \end{array}\right) \tag{34}$$

$$\dot{b_1} = \frac{-3}{8}\left(\begin{array}{l} 4q_3^2\sin(u) + 16q_3\sin(2u)a_1 + 6\sin(u){a_1}^2 + 14\sin(3u){a_1}^2 + 3\sin(u){a_2}^2 \\ -\sin(3u){a_2}^2 + 32q_3\cos(u)a_3 + 16a_1a_3 + 48\cos(2u)a_1a_3 - 32\sin(u){a_3}^2 \\ +16q_3\cos(2u)b_1 + 4\cos(u)a_1b_1 + 28\cos(3u)a_1b_1 - 48\sin(2u)a_3b_1 \\ +2\sin(u){b_1}^2 - 14\sin(3u){b_1}^2 + 2\cos(u)a_2b_2 - 2\cos(3u)a_2b_2 \\ +\sin(u){b_2}^2 + \sin(3u){b_2}^2 \end{array}\right) \tag{35}$$

$$\dot{b_2} = \frac{3}{4}\left(\begin{array}{l} -3\sin(u)a_1a_2 + \sin(3u)a_1a_2 - 4a_2a_3 + y4\cos(2u)a_2a_3 - \cos(u)a_2b_1 \\ +\cos(3u)a_2b_1 - \cos(u)a_1b_2 + \cos(3u)a_1b_2 - 4\sin(2u)a_3b_2 - \sin(u)b_1b_2 \\ -\sin(3u)b_1b_2 \end{array}\right) \tag{36}$$

$$\dot{q_3} = \frac{-3}{2}\left(\begin{array}{l} 2q_3^2 + 2{a_1}^2 + {a_2}^2 + 2a_3 - 16\sin(u)a_1a_3 - 16{a_3}^2 - 8q_3\sin(u)b_1 \\ -12\sin(2u)a_1b_1 + 2{b_1}^2 + 8\cos(u)\left(q_3a_1 - 2a_3b_1\right) + 2\sin(2u)a_2b_2 \\ +{b_2}^2 + \cos(2u)(2u)(3u)\left(6{a_1}^2 - {a_2}^2 - 6{b_1}^2 + {b_2}^2\right) \end{array}\right) \tag{37}$$

Recall that for the first-order solution, the condition for a bounded relative motion was $a_3 = 0 = \dot{y} + 2x$. Here, where we include the effect of the higher-order terms, we can find a new condition for boundedness that is second-and third-order in the initial conditions. We do this by solving the variational equations above using a Poincarè-Lindstedt procedure. We add to the epicyclic elements small, time varying perturbations that solve Eqs. (32) - (37). These small, time varying terms are going to be second-and third-order in the initial conditions. The second-order terms, for example, are found by plugging in the first-order, constant values (zero for a_3) into Eqs. (32) - (37) and integrating by quadrature. Doing so we find that all of the epicyclic elements are periodic except for q_3. However, by setting the non-periodic part of q_3 equal to zero we find a new condition on $a_3(0)$

to ensure bounded relative motion,

$$a_3(0) = -\frac{5}{2}a_1^2(0) - \frac{1}{2}(a_2^2(0) - b_1^2(0) + b_2^2(0)) - 3a_1(0)b_3(0) - b_3^2(0) \tag{38}$$

Our boundedness condition now consists of second-order powers of the initial conditions. The resulting solution for $(a_1(u), b_1(u), a_2(u), b_2(u), a_3(u), q_3(u))$ is substituted back into the Cartesian Eqs. (28) - (30) to find the complete second-order solution. We follow the same procedure for the third-order perturbation term, though the variational equations are too cumbersome to reproduce here. The boundedness condition then becomes,

$$\begin{aligned} a_3(0) &= -\frac{5}{2}a_1^2(0) - \frac{1}{2}(a_2^2(0) - b_1^2(0) + b_2^2(0)) - 3a_1(0)b_3(0) - b_3^2(0) \\ &\quad -\frac{3}{2}(a_1^2(0)b_1(0) + a_2^2(0)b_1(0)) + \frac{1}{2}b_1^3(0) \end{aligned} \tag{39}$$

Again, the full third-order solution can then be found via substitution. Figure 2 shows a pseudo-elliptical relative orbit in the Hill frame using the above initial boundedness condition. The parameters and initial conditions were chosen to compare to the similar result in [9]. The reference orbit has an altitude of 1700 km and the relative motion extends 20 km in y (and 40 km in x) and roughly 5 km out-of-plane in z. The drift of this orbit is roughly 1 cm per orbit, compared to hundreds of meters per orbit using only the first-order condition (the CW solution). Fig. 3 shows the difference between this full, nonlinear simulation and the third-order variational solution.

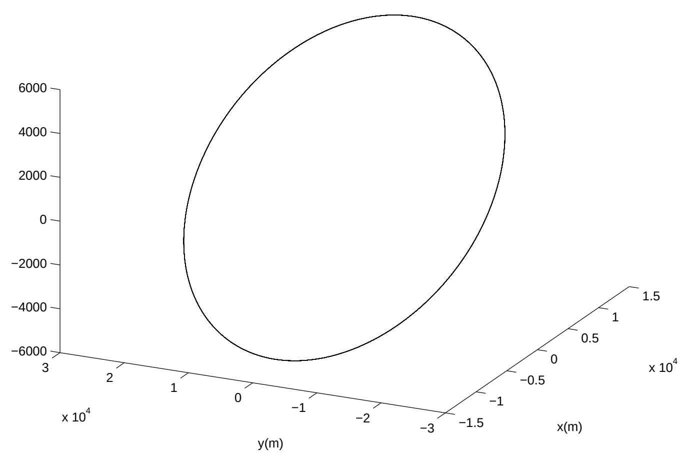

Figure 2. Exact nonlinear simulation of 3-dimensional relative orbit using the third-order boundedness condition. Total drift of the trajectory is less than 1 cm per orbit.

4. J_2 PERTURBATION

In Ref. [6] we go into some detail on using this approach to studying the perturbation of a relative motion trajectory due to the J_2 oblateness. We therefore only summarize the results here. For illustration, it is simpler to begin with the restricted case of a circular, equatorial reference orbit and follow the perturbation analysis as above. The perturbing Hamiltonian is,

$$\mathcal{H}^{(1)} = \frac{n^2 J_2 R_\oplus^2 (2z^2 - 1 - 2x - x^2 - y^2)}{2a^2(1 + 2x + x^2 + y^2 + z^2)^{(5/2)}} \tag{40}$$

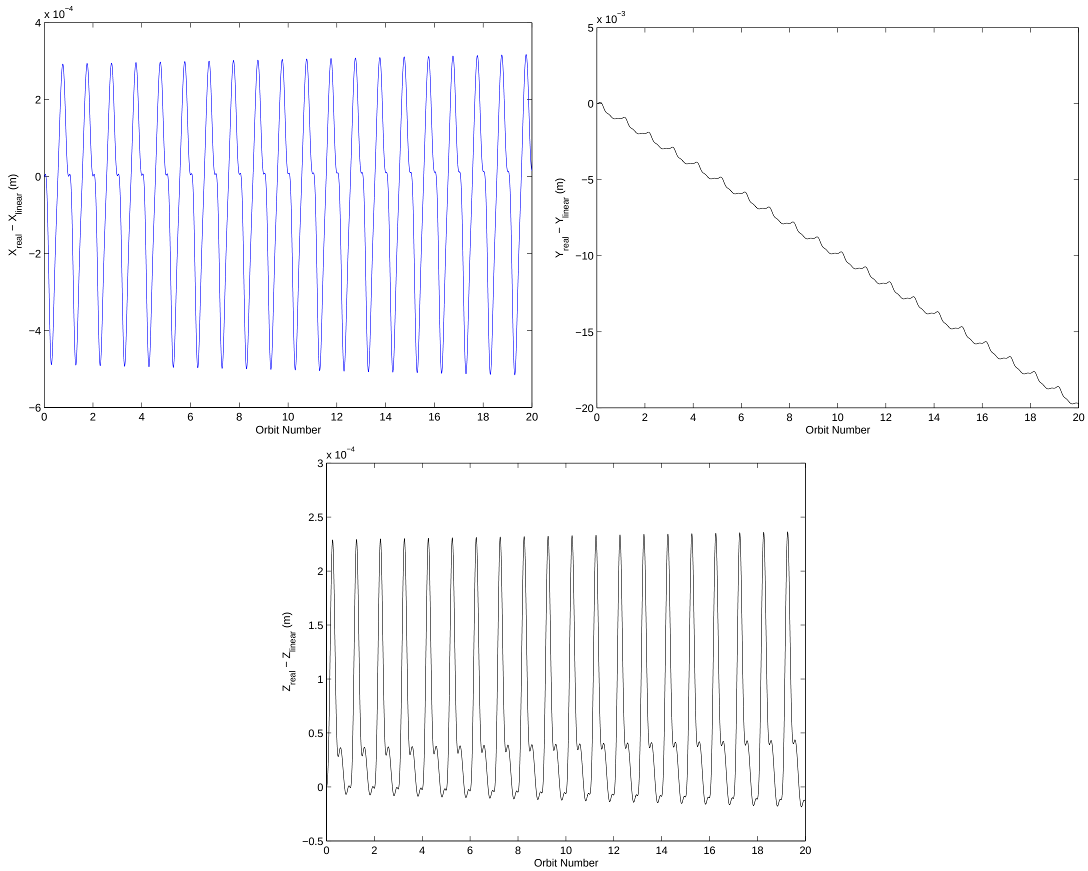

Figure 3. Difference between exact nonlinear simulation and the third-order variational solution.

where we have again normalized distances by the reference orbit radius, a. This is expanded to second-order and (x, y, z) is replaced by their time varying solution in terms of the epicyclic elements. Hamilton's equations are then used to find the variational equations for the elements, which, in terms of the contact elements, are,

$$\dot{a}_1 = \frac{3}{2}J_2\left(\frac{R_\oplus}{a}\right)^2\begin{pmatrix} -\cos(u-u_0)+4\sin(2(u-u_0))a_1 \\ +4\cos(2(u-u_0))b_1+2\sin(u-u_0)q_3 \\ +8\cos(u-u_0)a_3 \end{pmatrix} \tag{41}$$

$$\dot{b}_1 = \frac{3}{2}J_2\left(\frac{R_\oplus}{a}\right)^2\begin{pmatrix} \sin(u-u_0)+4\cos(2(u-u_0))a_1 \\ -4\sin(2(u-u_0))b_1+2\cos(u-u_0)q_3 \\ -8\sin(u-u_0)a_3 \end{pmatrix} \tag{42}$$

$$\dot{a}_2 = -\frac{9}{4}J_2\left(\frac{R_\oplus}{a}\right)^2((1+\cos(2(u-u_0)))b_2-\sin(2(u-u_0))a_2) \tag{43}$$

$$\dot{b}_2 = \frac{9}{4}J_2\left(\frac{R_\oplus}{a}\right)^2(\sin(2(u-u_0))b_2-(1-\cos(2(u-u_0)))a_2) \tag{44}$$

$$\dot{a}_3 = -\frac{3}{2}J_2\left(\frac{R_\oplus}{a}\right)^2(q_3+2\cos(u-u_0)a_1-2\sin(u-u_0)b_1) \tag{45}$$

$$\dot{q}_3 = -3a_3+3J_2\left(\frac{R_\oplus}{a}\right)^2\begin{pmatrix} 1-8a_3-4\sin(u-u_0)a_1 \\ -4\cos(u-u_0)b_1 \end{pmatrix} \tag{46}$$

Since we are performing our analysis to first-order in J_2 only and we assume small relative motion, these can be simplified in a low-order analysis to,

$$\dot{a}_1 = -\frac{3}{2}J_2\left(\frac{R_\oplus}{a}\right)^2\cos(u-u_0) \tag{47}$$

$$\dot{b}_1 = \frac{3}{2}J_2\left(\frac{R_\oplus}{a}\right)^2\sin(u-u_0) \tag{48}$$

$$\dot{a}_2 = 0 \tag{49}$$

$$\dot{b}_2 = 0 \tag{50}$$

$$\dot{a}_3 = 0 \tag{51}$$

$$\dot{q}_3 = -3a_3 + 3J_2\left(\frac{R_\oplus}{a}\right)^2 \tag{52}$$

These equations can be easily solved by quadrature,

$$a_1 = a_1(0) - \frac{3}{2}J_2\left(\frac{R_\oplus}{a}\right)^2\sin(u-u_0) \tag{53}$$

$$b_1 = b_1(0) - \frac{3}{2}J_2\left(\frac{R_\oplus}{a}\right)^2\cos(u-u_0) \tag{54}$$

$$a_2 = a_2(0) \tag{55}$$

$$b_2 = b_2(0) \tag{56}$$

$$a_3 = a_3(0) \tag{57}$$

$$q_3 = q_3(0) + 3(J_2\left(\frac{R_\oplus}{a}\right)^2 - a_3(0))(u-u_0) \tag{58}$$

In order to eliminate the along-track drift, we set $a_3(0) = J_2\left(\frac{R_\oplus}{a}\right)^2$. If we also simplify by considering only in-plane motion (by setting $a_2(0) = b_2(0) = 0$), then inserting these solutions back into Eqs. (28) - (30) shows that one equilibrium solution consists of a constant radial offset of $x = \frac{J_2}{2}\left(\frac{R_\oplus}{a}\right)^2$. This is the same as the well known result for the needed constant radial offset to establish a circular, equatorial orbit in the presence of J_2 (most simply found by equating the gravitational and centrigual forces). This is a convincing validation of the approach.

The true power of the technique is displayed for the general J_2 perturbation problem. Here we find a very simple periodic relative motion condition for any reference orbit at all inclinations. However, to do so we must introduce one complication. We know from the perturbed two-body problem that any satellite orbit will have a long term, secular drift in the node angle and argument of perigee induced by oblateness. Thus, it is clearly impossible, using any technique, to find a boundedness condition for motion relative to a fixed reference orbit (and, of course, the drift will quickly invalidate the small motion assumption). One approach is to treat the perturbation inertially. Schaub and Alfriend [10, 8], for example, realizing this, derived general J_2–invariant (and almost invariant) satellite formations by matching the drifts among the satellites. In other words, the satellite orbits still drift relative to the usual Hill reference frame, but they drift in such a way that the formation remains bounded. Unfortunately, this loses the advantage provided by the relative frame description and tends to have singularity problems.

To solve the problem in our canonical formalism, we return to the original solution of the H-J equation and replace the fixed, Hill-like reference orbit with a circular orbit that also rotates at the mean J_2 induced drift rate. Thus, the new reference frame, rather than rotating only about the z-axis at the nominal orbit rate, now has the more complicated angular velocity,

$$^{\mathscr{I}}\boldsymbol{\omega}^{\mathscr{R}} = \begin{bmatrix} \dot{\Omega}\sin i \sin u \\ \dot{\Omega}\sin i \cos u \\ \dot{\Omega}\cos i + \dot{u} \end{bmatrix}_{\mathscr{I}} \tag{59}$$

where u is the argument of latitude, $\dot{u} = n + \delta n$ is the modified orbit rate including the J_2 perturbation, and $n = \sqrt{\mu/\bar{a}^3}$, $\bar{a}$ being the mean semi-major axis. The equations for the drift rates are somewhat subtle, as the usual expressions are written in terms of the initial or mean semi-major axis of the osculating orbit (see, e.g., [11] or [13]). Here, however, we select a circular reference orbit with the radius, $\bar{r}$, equivalent to the mean radius of the J_2 perturbed orbit [12],

$$\bar{r} = \bar{a} + \frac{3}{4}J_2\left(\frac{R_\oplus}{\bar{a}}\right)^2(3\sin^2 i - 2) \tag{60}$$

Since we are free to select the reference orbit, this equation is solved for $\bar{a}$ and then used to find the mean rates of change of the node angle and argument of latitude [12, 13] for the arbitrary, circular reference orbit,

$$\dot{\Omega} = -\frac{3}{2}\bar{n}J_2\left(\frac{R_\oplus}{\bar{r}}\right)^2\cos i \tag{61}$$

$$\delta n = \frac{3}{4}\bar{n}J_2\left(\frac{R_\oplus}{\bar{r}}\right)^2\left(3 - \frac{7}{2}\sin^2 i\right) \tag{62}$$

where $\bar{n} = \sqrt{\mu/\bar{r}^3}$. Note also that in Eq. (62) we have included in $\dot{u}$ both the effect of the rate of change of true anomaly and of the argument of perigee as the reference orbit is circular (i.e., $\dot{u} = \dot{M} + \dot{\omega}$).

This angular velocity is then used to find the inertial velocity of the satellite and then kinetic and potential energies. This results in the new, normalized Lagrangian,

$$\begin{aligned} \bar{\mathcal{L}} &= \frac{1}{2}|\mathbf{v}^{(0)}|^2 + \mathbf{v}^{(0)}\cdot\mathbf{v}^{(1)} + \frac{1}{2}|\mathbf{v}^{(1)}|^2 \\ &\quad + \sum_{k=0}^{\infty} P_k(\cos\alpha)\rho^k - \bar{U}_{zonal} \end{aligned} \tag{63}$$

where $\mathbf{v}^{(0)}$ is the part of the normalized velocity in the relative motion frame independent of J_2 (and the same as the velocity in the original problem),

$$\mathbf{v}^{(0)} = \begin{bmatrix} \dot{x} - y \\ \dot{y} + (x+1) \\ \dot{z} \end{bmatrix} \tag{64}$$

and $\mathbf{v}^{(1)}$ is the small remaining term of order J_2,

$$\mathbf{v}^{(1)} = \begin{bmatrix} v_x^{(1)} \\ v_y^{(1)} \\ v_z^{(1)} \end{bmatrix} = \begin{bmatrix} \bar{\dot{\Omega}}s_i c_u z - (\bar{\dot{\Omega}}c_i - \bar{\delta n})y \\ (\bar{\dot{\Omega}}c_i - \bar{\delta n})(x+1) - \bar{\dot{\Omega}}s_i s_u z \\ \bar{\dot{\Omega}}s_i s_u y - \bar{\dot{\Omega}}s_i c_u(x+1) \end{bmatrix} \tag{65}$$

where $\bar{\dot{\Omega}} = \dot{\Omega}/\bar{n}$ and $\bar{\delta n} = \delta n/\bar{n}$.

As we did before, we can expand this Lagrangian and keep only the low order terms (including terms to first-order only in J_2). This allows us to drop the second-order term, $\frac{1}{2}|\mathbf{v}^{(1)}|^2$, and rewrite the Lagrangian,

$$\bar{\mathcal{L}} = \bar{\mathcal{L}}^{(0)} + \mathbf{v}^{(0)}\cdot\mathbf{v}^{(1)} - \bar{U}_{zonal} \tag{66}$$

where we are ignoring the second-order terms of the previous section. It is interesting to note that this Lagrangian could be used in the Euler-Lagrange equations to find second-order equations of motion in this new rotating and drifting frame, which may have some usefulness for control design.

With this Lagrangian, we compute the new canonical momenta,

$$\begin{aligned} p_x &= \frac{\partial \bar{\mathcal{L}}}{\partial \dot{x}} = \dot{x} - y + v_x^{(1)} \\ p_y &= \frac{\partial \bar{\mathcal{L}}}{\partial \dot{y}} = \dot{y} + x + 1 + v_y^{(1)} \\ p_z &= \frac{\partial \bar{\mathcal{L}}}{\partial \dot{z}} = \dot{z} + v_z^{(1)} \end{aligned} \tag{67}$$

and, again using the Legendre transformation, $\mathcal{H} = \sum \dot{q}_i p_i - L$, we find the new Hamiltonian,

$$\begin{aligned} \mathcal{H} &= \frac{1}{2}(p_x + y - v_x^{(1)})^2 + \frac{1}{2}(p_y - (x+1) - v_y^{(1)})^2 + \frac{1}{2}(p_z - v_z)^2 \\ &\quad -\frac{3}{2} - \frac{3}{2}x^2 + \frac{1}{2}z^2 + yv_x^{(1)} - (x+1)v_y^{(1)} + \bar{U}_{zonal} \end{aligned} \tag{68}$$

Multiplying out the terms in Eq. (68) results in the same low order Hamiltonian, $\mathcal{H}^{(0)}$, as the original problem and the perturbing Hamiltonian,

$$\mathcal{H}^{(1)} = -p_x v_x^{(1)} - p_y v_y^{(1)} - p_z v_z^{(1)} + \bar{U}_{zonal} \tag{69}$$

where we have again dropped terms of second-order (or higher) in J_2. The solution to the H-J equation is the same as before, with the Cartesian relative motion given by Eqs. (28) - (30) in terms of the contact epicyclic elements, only now the motion is referred to the rotating and drifting reference orbit. However, due to the modified definition of the canonical momenta, the cartesian rates are slightly different,

$$\dot{x}(u) = a_1 \cos(u - u_0) - b_1 \sin(u - u_0) - v_x^{(1)} \tag{70}$$

$$\dot{y}(u) = -3\alpha_3 - 2a_1 \sin(u - u_0) - 2b_1 \cos(u - u_0) - v_y^{(1)} \tag{71}$$

$$\dot{z}(u) = a_2 \cos(u - u_0) - b_2 \sin(u - u_0) - v_z^{(1)} \tag{72}$$

and the relationship between the elements and Cartesian initial conditions are likewise modified.

This formalism results in a rather unique form for the perturbing Hamiltonian in Eq. (69); that is, $\mathcal{H}^{(1)}$ depends upon the canonical momenta and velocities. It is shown in [14, 15] that for problems where the perturbing Hamiltonian is velocity dependent, the resulting instantaneous trajectory (Eqs. (28)-(30)) is not osculating. While the physical trajectory we find will be exact (and quite useful), we must therefore keep in mind that it is not formed from a series of tangent ellipses as in the other perturbation cases we are examining or as in the Delaunay formulation of the two-body problem. An alternative approach is to resolve the H-J equation for the new canonical momenta; this is a formidable task, however, and we defer to future work.

As before, we form the perturbing Hamiltonian and use Hamilton's equations to find the variational equations, which, to first-order in J_2 and the contact elements, are,

$$\dot{a}_1 = -\frac{3}{32}J_2\left(\frac{R_\oplus}{\bar{r}}\right)^2\begin{pmatrix} \cos(2i-u-u_0)-7\cos(3u-u_0+2i) \\ +14\cos(3u-u_0)+6\cos(u-u_0-2i) \\ +4\cos(u-u_0)-7\cos(3u-u_0-2i) \\ +6\cos(u-u_0+2i)-2\cos(u+u_0) \\ +\cos(u+u_0+2i) \end{pmatrix} \quad (73)$$

$$\dot{b}_1 = \frac{3}{32}J_2\left(\frac{R_\oplus}{\bar{r}}\right)^2\begin{pmatrix} -\sin(u+u_0+2i)-\sin(u+u_0-2i) \\ +14\sin(3u-u_0)-7\sin(3u-u_0+2i) \\ -7\sin(3u-u_0-2i) \\ +6\sin(u-u_0-2i)+6\sin(u-u_0+2i) \\ +2\sin(u+u_0)+4\sin(u-u_0) \end{pmatrix} \quad (74)$$

$$\dot{a}_2 = \frac{3}{8}J_2\left(\frac{R_\oplus}{\bar{r}}\right)^2(\cos(2u-u_0+2i)-\cos(2u-u_0-2i)) \quad (75)$$

$$\dot{b}_2 = -\frac{3}{8}J_2\left(\frac{R_\oplus}{\bar{r}}\right)^2(\sin(2u-u_0+2i)-\sin(2u-u_0-2i)) \quad (76)$$

$$\dot{a}_3 = -\frac{3}{8}J_2\left(\frac{R_\oplus}{\bar{r}}\right)^2(\sin(2u-2i)+\sin(2u+2i)-2\sin(2u)) \quad (77)$$

$$\dot{q}_3 = -3a_3-\frac{9}{16}J_2\left(\frac{R_\oplus}{\bar{r}}\right)^2\begin{pmatrix} 4\cos(2u)-2\cos(2u-2i) \\ -2\cos(2u+2i)+3\cos(2i)+1 \end{pmatrix} \quad (78)$$

As in the equatorial case, these equations can easily be solved by quadrature. We again find a secular drift term proportional to $a_3(0)$. However, because of our careful selection of the drifting reference orbit, we are able to find a straightforward boundedness condition,

$$a_3(u_0) = \frac{3}{16}J_2\left(\frac{R_\oplus}{\bar{r}}\right)^2\begin{bmatrix} 1+3\cos(2i)+2\cos(2u_0) \\ -\cos(2i-2u_0)-\cos(2i+2u_0) \end{bmatrix} \quad (79)$$

Substituting this condition into the solution for the elements and then into the Cartesian generating equations result in the periodic equations for the relative motion trajectory,

$$x(u) = a_1(u_0)\sin(u-u_0)+b_1(u_0)\cos(u-u_0) + \frac{1}{32}J_2\left(\frac{R_\oplus}{\bar{r}}\right)^2\begin{pmatrix} 4\cos(2u)-2\cos(2u+2i)-2\cos(2u-2i) \\ +12\cos(u-u_0)+6\cos(u+u_0) \\ +18\cos(u-u_0-2i)+18\cos(u-u_0+2i) \\ -3\cos(u+u_0-2i)-3\cos(u+u_0+2i) \\ +14\cos(u-3u_0) \\ -7\cos(u-3u_0+2i)-7\cos(u-3u_0-3i) \end{pmatrix} \quad (80)$$

$$y(u) = q_3(u_0)+2a_1(u_0)\cos(u-u_0)-2b_1(u_0)\sin(u-u_0) + \frac{1}{32}J_2\left(\frac{R_\oplus}{\bar{r}}\right)^2\begin{pmatrix} 2\sin(2u)-\sin(2u-2i)-\sin(2u+2i) \\ -24\sin(u-u_0)-12\sin(u+u_0)-18\sin(2u_0) \\ +9\sin(2u_0+2i)+9\sin(2u_0-2i) \\ -36\sin(u-u_0-2i)-36\sin(u-u_0+2i) \\ +6\sin(u+u_0-2i)+6\sin(u+u_0+2i) \\ -28\sin(u-3u_0) \\ +14\sin(u-3u_0+2i)+14\sin(u-3u_0-2i) \end{pmatrix} \quad (81)$$

$$z(u) = a_2(u_0)\sin(u-u_0)+b_2(u_0)\cos(u-u_0) + \frac{3}{16}J_2\left(\frac{R_\oplus}{\bar{r}}\right)^2\begin{pmatrix} \cos(u+2i)-\cos(u-2i) \\ +\cos(u-2u_0+2i)-\cos(u-2u_0-2i) \end{pmatrix} \quad (82)$$

Once again, these can be verified by examining the constant offset at $i = 0$ and we again find the correct result.

In [6] we present simulations of periodic relative motion trajectories for three different inclinations. For brevity, we present only one of those here. For these simulations, we selected initial conditions on the contact epicyclic elements (with the boundedness condition on $a_3(0)$ from Eq. (79)) and then found the cartesian initial conditions in the rotating and drifting frame from,

$$x(u_0) = 2a_3(u_0) + b1(u_0) \tag{83}$$

$$y(u_0) = q_3(u_0) + 2a_1(u_0) \tag{84}$$

$$z(u_0) = b_2(u_0) \tag{85}$$

and the initial rates from Eqs. (70) - (72),

$$\dot{x}(u_0) = a1_(u_0) - v_x^{(1)}(u_0) \tag{86}$$

$$\dot{y}(u_0) = -3a_3(u_0) - 2b_1(u_0) - v_y^{(1)}(u_0) \tag{87}$$

$$\dot{z}(u_0) = a_2(u_0) - v_z^{(1)}(u_0) \tag{88}$$

These initial conditions were then rotated and translated into an inertial frame for a full nonlinear simulation. The circular reference orbit selected had an altitude of 750 km. All the initial conditions on the contact elements were set to zero except for $a_3(0)$.

Figure 4 shows an example of a bounded relative motion over 5 orbits including J_2 effects relative to a sun-synchronous reference orbit. Also in this figure is the difference between the full nonlinear simulation and the relative motion from Eqs. (80)-(82). [‡] The boundedness condition works quite well, resulting in an average drift of roughly 20 m/orbit. However, this may still be considered too large (the residual resulting from neglected terms of $\mathcal{O}(J_2^2)$). Remarkably, this drift can be fairly easily reduced via a simple iteration of the nonlinear initial conditions. By using the no-drift condition as a starting point, we find a slight modification of the relative motion initial in-track velocity that significantly reduces the in-track drift in only 5 iterations. By changing the initial in-track velocity by just less than 0.006 m/s we can reduce the orbit drift to less than 5 meters/orbit. Such an orbit is shown in Fig. 5.

5. ECCENTRIC REFERENCE ORBITS

For our last example, we find bounded relative motion trajectories relative to a slightly elliptical reference orbit. A number of researchers have looked at the problem of relative motion relative to elliptical orbits [16, 17]. Most have have approached the problem by solving for the motion in terms of true anomaly rather than time. Here, we treat the eccentricity as a small perturbation and solve for the deviation of our 2:1 elliptical solution due to small eccentricity. We note that in [18] we used the same approach to study elliptic orbit perturbations on relative motion. However, there were a number of errors in that work, particularly in the treatment of averaging; what we present below should be referenced instead.

For the eccentric orbit problem, we use the same reference frame as in Fig. 1 but here rotating at the time varying rate, $\dot{\theta}(\theta)$, where θ is the true anomaly. Letting $r_c(\theta) = |\mathbf{r}_1|$, the velocity becomes,

$$\mathbf{v} = \begin{bmatrix} \dot{x} + \dot{r}_c(\theta) - \dot{\theta}y \\ \dot{y} + \dot{\theta}(x + r_c(\theta)) \\ \dot{z} \end{bmatrix} \tag{89}$$

[‡]This figure shows the geometric difference between the two orbits. Plots of the difference in the Cartesian components show a large, and growing, oscillation due a slight difference in the rates and thus a growing offset in phasing. See [6] for details.

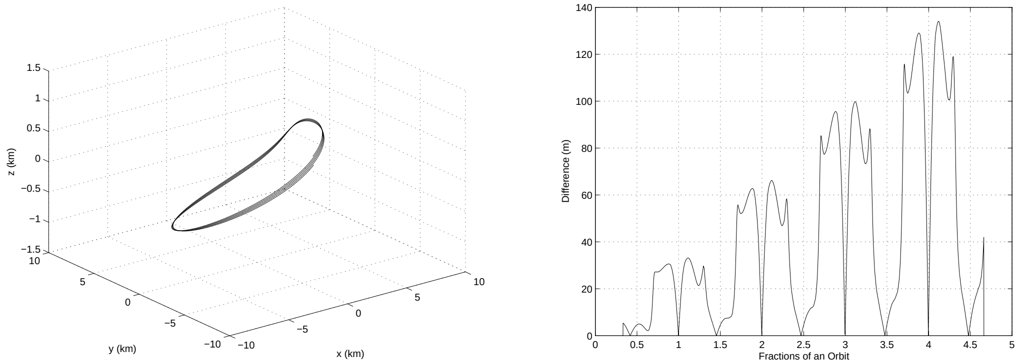

Figure 4. *Left* Nonlinear simulation of bounded relative motion trajectory in a sun-synchronous reference orbit. *Right* A comparison of the relative displacement between the linearized trajectory and that from a full, inertial, nonlinear simulation over 5 orbits for a Sun-Synchronous reference orbit.

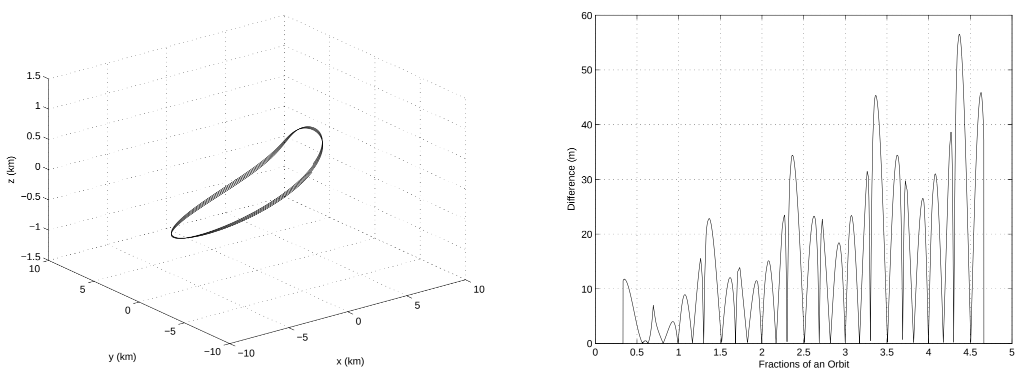

Figure 5. Nonlinear simulation of bounded, minimal drift relative motion trajectory in a sun-synchronous reference orbit.

As before, we can use this velocity in the kinetic energy to find the normalized, perturbed Lagrangian,

$$\mathcal{L} = \frac{1}{2}\{(\dot{x} + \dot{r}_c - \dot{\theta}\ y)^2 + (\dot{y} + \dot{\theta}(x + r_c))^2 + \dot{z}^2\} + \frac{1}{r_c} - \frac{x}{r_c^2} + \frac{1}{2r_c^3}(2x^2 - y^2 - z^2) \tag{90}$$

where again we have included only the low-order terms in the potential. As in the J_2 problem, we find new canonical momenta,

$$\begin{aligned} p_x &= \frac{\partial L}{\partial \dot{x}} = \dot{x} + \dot{r}_c(\theta) - y\dot{\theta} \\ p_y &= \frac{\partial L}{\partial \dot{y}} = \dot{y} + x\dot{\theta} + r_c(\theta)\dot{\theta} \\ p_z &= \frac{\partial L}{\partial \dot{z}} = \dot{z} \end{aligned} \tag{91}$$

and the resulting normalized Hamiltonian,

$$\mathcal{H} = \frac{1}{2}(p_x^2 + p_y^2 + p_z^2) + p_x(-\dot{r}_c + y\dot{\theta}) - p_y(r_c + x)\dot{\theta} - \frac{1}{r_c} + \frac{x}{r_c^2} + \frac{1}{2r_c^3}(-2x^2 + y^2 + z^2) \tag{92}$$

Note that θ and r_c are not independent variables, but rather predetermined functions of time and initial conditions.

The Hamilton-Jacobi equation for this system is unsolvable. However, when the eccentricity is small, the eccentric Hamiltonian approaches the circular Hamiltonian. As a result, we can conceive of the eccentric motion as a perturbation of the motion relative to a circular orbit of the same period. This allows us to use the same formalism as in our other examples. The nominal motion is given as the same solution as before (Eqs. (28) - (30)). The effect of eccentricity is then found via the variations due to the perturbing Hamiltonian, $H^{(1)}$,

$$\begin{aligned} H^{(1)} &= H - H^{(0)} \\ &= 1 + p_y - \frac{1}{r_c} - x + p_y x + \frac{x}{r_c^2} + x^2 - \frac{x^2}{r_c^3} - p_x y \\ &\quad -\frac{y^2}{2} + \frac{y^2}{2r_c} - \frac{z^2}{2} + \frac{z^2}{2r_c} - p_x \dot{r}_c - \left(p_y\left(r_c + x\right) - p_x y\right)\dot{\theta} \end{aligned} \tag{93}$$

As in the J_2 case, this Hamiltonian is velocity dependent; thus, the instantaneous trajectories are again not osculating to the true trajectory.

By again substituting for (x, y, z, p_x, p_y, p_z) and using Hamilton's equations, it is possible to find the variation equations. However, our aim is to find the trajectory evolution of the system across time, requiring us to find the time dependence of $r_c(\theta(t))$ and $\theta(t)$,

$$r_c = 1 - e\cos E \tag{94}$$

$$\tan(\frac{\theta}{2}) = \sqrt{\frac{1+e}{1-e}}\tan(\frac{E}{2}) \tag{95}$$

where E, the eccentric anomaly, is obtained from Kepler's Equation,

$$M = n(t-\tau) = E - e\sin E \tag{96}$$

Since Kepler's equation cannot be solved explicitly for time, we adopt the Fourier-Bessel series solution from [11] and express r_c and θ in terms of eccentricity and time as follows,

$$\theta = M + 2\sum_{k=1}^{\infty}\frac{1}{k}\left[\sum_{n=-\infty}^{\infty} J_n(-ke)\left(\frac{1-\sqrt{1-e^2}}{e}\right)^{|k+n|}\right]\sin(kM) \tag{97}$$

$$r_c = 1 + \frac{e^2}{2} - 2e\sum_{k=1}^{\infty}\frac{1}{k^2}\frac{dJ_k(ke)}{de}\sin(kM) \tag{98}$$

To find an expression for the variation of parameters caused by the eccentric reference orbit, we substitute for r_c and θ from Eqs. (97) and (98) in the expression for $H^{(1)}$ in Eq. (93) and expand up to second-order in e,

$$\begin{aligned} H^{(1)} &= \frac{e}{2}\left[\left(-2 + 4x - 6x^2 - 2p_y\left(1+2x\right) + 4p_x y + 3y^2 + 3z^2\right)\cos\left(M\right) - 2p_x\sin\left(M\right)\right] \\ &\quad + \frac{e^2}{4}\left[\begin{array}{l} 2p_y + 2x - 6x^2 + 3y^2 + 3z^2 + \\ \left(-4 + 10x - 2p_y\left(2+5x\right) + 10p_x y - 18x^2 + 9y^2 + 9z^2\right)\cos\left(2M\right) \\ -4p_x\sin\left(2M\right) \end{array}\right] \\ &\quad + \mathcal{O}\left(e^3\right) \end{aligned} \tag{99}$$

Using the usual series of transformations to change from (x, y, z, p_x, p_y, p_z) to $(a_1, a_2, a_3, b_1, b_2, b_3)$

and applying Hamilton's equations results in the variational equations to first-order in e,

$$\begin{aligned}
\dot{a}_1 &= -e\cos(2M - M_0) && (100)\\
\dot{a}_2 &= 0 && (101)\\
\dot{a}_3 &= -e\sin(M) && (102)\\
\dot{b}_1 &= e\sin(2M - M_0) && (103)\\
\dot{b}_2 &= 0 && (104)\\
\dot{q}_3 &= -3a_3 + e\cos(M) && (105)
\end{aligned}$$

These equations are easily solved by quadrature to yield,

$$\begin{aligned}
a_1 &= a_1(0) + \frac{e}{2}(-\sin(2M - M_0) + \sin(M_0)) && (106)\\
a_2 &= a_2(0) && (107)\\
a_3 &= a_3(0) + e(\cos(M) - \cos(M_0)) && (108)\\
b_1 &= b_1(0) + \frac{e}{2}(-\cos(2M - M_0) + \cos(M_0)) && (109)\\
b_2 &= b_2(0) && (110)\\
q_3 &= b_3(0) + (M - M_0)(-3a_{30} + 3e\cos(M_0)) + e(-2\sin(M) + 2\cos(M_0)) && (111)
\end{aligned}$$

The boundedness condition in this case is that $a_3(0) = e\cos(M_0)$. Relative motion is extremely sensitive to very slight eccentricities of the reference orbit. Using only the CW equations with an eccentricity of only 0.001 results in a drift of many hundreds of meters per orbit. This first-order condition alone makes a great improvement, but the drift can still be many tens of meters per orbit. It is necessary, and straightforward, to include higher-order eccentricity terms. However, the resulting perturbations become of the same order as the higher-order nonlinear effects and thus cannot be considered separately. We present this combined effect in the next section.

6. COMBINED PERTURBATIONS

Because each of these perturbations appear as an added term in the Hamiltonian, the combined effects are found by simply summing the variations. As mentioned above, when going to higher-order in e, for example, the variations must be combined with the higher-order nonlinearities as the errors are of the same order for reasonably sized relative trajectories. The variational equations that result are too long to present here, but the boundedness condition for the third-order combined effects becomes,

$$\begin{aligned}
a_3(0) &= e\cos(M_0) + \frac{e^2}{8}\begin{pmatrix} -2 - 20\tilde{a}_1^2(0) - 4\tilde{a}_2^2(0) + 4\tilde{b}_1^2(0) - 4\tilde{b}_2^2(0) \\ -24\tilde{a}_1(0)\tilde{b}_3(0) - 8\tilde{b}_3^2(0) + 8\tilde{b}_1(0)\cos(M_0) + 6\cos(2M_0) \end{pmatrix} \\
&\quad + \frac{e^3}{4}\begin{pmatrix} \tilde{b}_1(0) - 6\tilde{a}_1^2(0)\tilde{b}_1(0) - 6\tilde{a}_2^2(0)\tilde{b}_1(0) + 2\tilde{b}_1^3(0) - 12\tilde{a}_1(0)\tilde{b}_1(0)\tilde{b}_3(0) \\ -6\tilde{b}_1(0)\tilde{b}_3^2(0) - \cos(M_0) - 6\tilde{a}_1^2(0)\cos(M_0) - 6\tilde{a}_2^2(0)\cos(M_0) \\ +6\tilde{b}_1^2(0)\cos(M_0) - 12\tilde{a}_1(0)\tilde{b}_3(0)\cos(M_0) - 6\tilde{b}_3^2(0)\cos(M_0) \\ +5\tilde{b}_1(0)\cos(2M_0) + 3\cos(3M_0) \end{pmatrix} && (112)
\end{aligned}$$

where $\tilde{a}_i(0) = a_i(0)/e$ and $\tilde{b}_i(0) = b_i(0)/e$.

Figure 6 shows a nonlinear simulation of a 3-dimensional relative motion trajectory about a reference orbit of eccentricity $e = 0.001$ and altitude 1700 km. The above combined boundedness condition was used, resulting in an overall drift of 1 to 2 mm/orbit. Figure 7 shows the difference between the nonlinear simulation and the combined third-order variational solution.

We can also combine, for example, the first-order eccentricity and J_2 perturbations to find the effect of oblateness on an eccentric reference orbit. The boundedness condition is simply the sum of

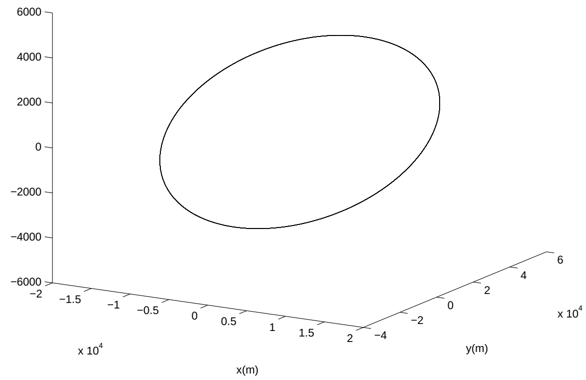

Figure 6. Exact nonlinear simulation of 3-dimensional relative orbit using the third-order boundedness condition on eccentricity and nonlinearity. Total drift of the trajectory is less than 1 cm per orbit.

Eq. (79) with the first-order eccentricity perturbation, $e\cos(M_0)$. While this works for very small eccentricity, it is not as effective for the eccentricities we are examining here. This is because the relative orbit drift rate is extremely sensitive to e (as we saw above) and higher-order corrections are needed. A proper combination, therefore, would have to include the $\mathcal{O}(J_2^2)$ terms as well. We postpone that to future work.

7. CONCLUSIONS AND FUTURE WORK

In this paper we summarized a new framework for modeling relative motion about circular and slightly eccentric reference orbits. We reformulate the well known 2:1 elliptical solution of the CW equations into a form dependent upon six canonical constants of the motion that are easily related to the Cartesian initial conditions in the rotating the frame. We then use canonical perturbation theory to find variational equations for these elements, which we termed "epicyclic", in direct analogy to the variation of the orbital elements. Not only does this approach provide straightforward, first-order differential equations of variation, but the description of the motion remains entirely in the relative motion frame, where most measurements are taken and where trajectory specification is most natural. In this paper we demonstrated the technique by finding conditions for bounded, periodic motion in the presence of higher-order nonlinearities, J_2 induced perturbations, and slight ellipticity of the reference orbit. In fact, we were able to find conditions for periodicity up to third-order in the relative positions and the eccentricity. We were also able to find a general expression for J_2 invariant orbits at any inclination and altitude.

There is much that can still be done to extend this methodology. In particular, we are interested in pursuing the combined effects including terms of $\mathcal{O}(J_2^2)$. We also intend to explore control techniques incorporating a control potential. Finally, we believe this approach can be fruitfully applied to motion about the co-linear Lagrange points in the circular restricted three-body problem.

References

[1] W.H. Clohessy and R.S. Wiltshire. Terminal guidance system for satellite rendezvous. *Journal of the Astronautical Sciences*, 27(9):653–678, September 1960.

[2] G.W. Hill. Researches in the lunar theory. *American Journal of Mathematics*, 1:5–26, 1878.

[3] H. Schaub, S.R. Vadali, and K.T. Alfriend. Formation flying control using mean orbital elements. *The Journal of the Astronautical Sciences*, 48(1):69–87, January-February 2000.

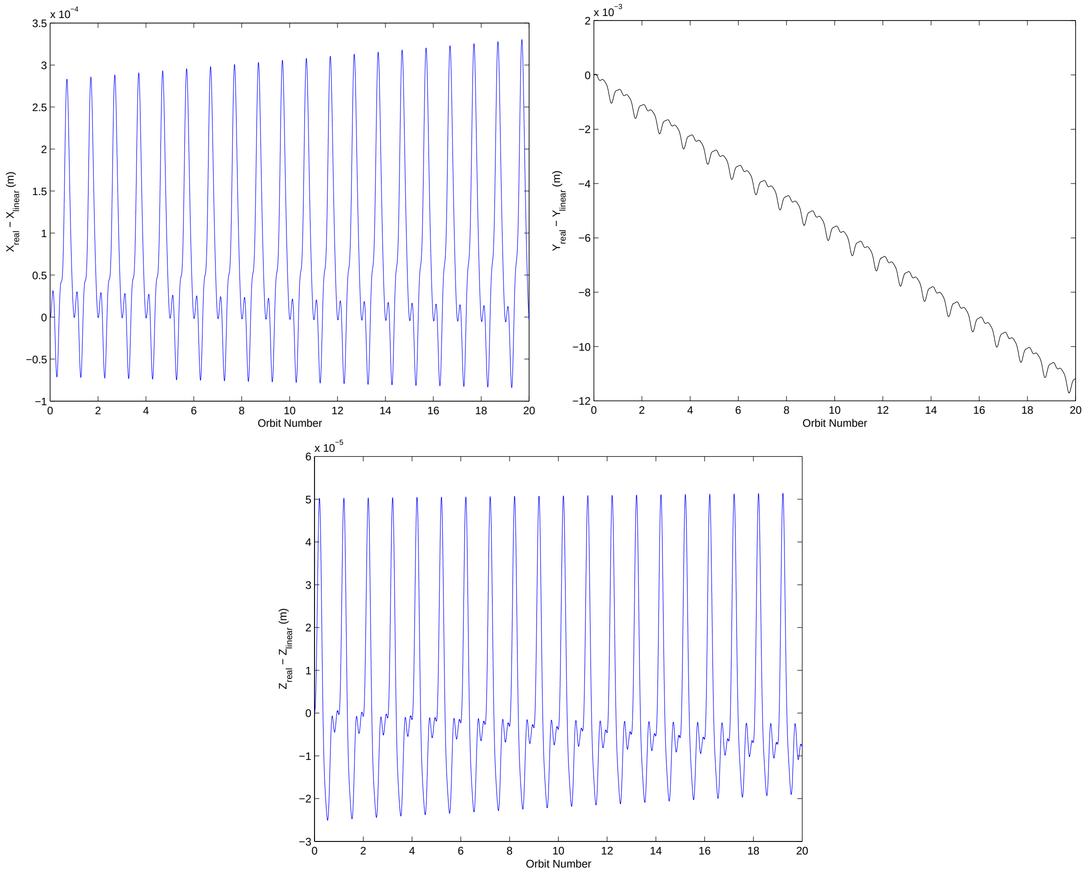

Figure 7. Difference between exact nonlinear simulation and the third-order variational solution.

[4] F. Namouni. Secular interactions of coorbiting objects. *Icarus*, 137:293–314, 1999.

[5] P. Gurfil and N.J. Kasdin. Nonlinear modeling and control of spacecraft relative motion in the configuration space. *Journal of Guidance, Control, and Dynamics*, 27(1):154–157, January 2004.

[6] N.J. Kasdin, P. Gurfil, and E. Kolemen. Canonical modelling of relative spacecraft motion via epicyclic orbital elements. *Celestial Mechanics and Dynamical Astronomy*, To Be Published, 2005.

[7] C.D. Karlgaard and F.H. Lutze. Second-order relative motion equations. In *Proceedings of the AAS/AIAA Astrodynamics Conference*, number AAS 01-464, July 2001. Quebec City, Quebec.

[8] K.T. Alfriend and H. Yan. An orbital elements approach to the nonlinear formation flying problem. In *International Formation Flying Symposium*, October 2002. Toulouse, France.

[9] D.L. Richardson and J.W. Mitchell. A third-order analytical solution for relative motion with a circular reference orbit. *The Journal of the Astronautical Sciences*, 51(1), January-February 2003.

[10] K.T. Alfriend and H. Schaub. Dynamics and control of spacecraft formations: Challenges and some solutions. *The Journal of the Astronautical Sciences*, 48(2):249–267, March-April 2000.

[11] RH. Battin. *An Introduction to the Mathematics and Methods of Astrodynamics*. AIAA, 1999.

[12] G. H. Born. Motion of a satellite under the influence of an oblate earth. Technical Report ASEN 3200, University of Colorado, Boulder, June 2001.

[13] J. P. Vinti. *Orbital and Celestial Mechanics*, volume 177 of *Progress in Astronautics and Aeronautics*. AIAA, 1998.

[14] M. Efroimsky and P. Goldreich. Gauge symmetry of the n-body problem in the hamilton-jacobi approach. *Journal of Mathematical Physics*, 44:5958–5977, 2003.

[15] M. Efroimsky and P. Goldreich. Gauge freedom in the n-body problem of celestial mechanics. *Astronomy and Astrophysics*, 415:1187–1899, 2004.

[16] T.E. Carter and M. Humi. Fuel-optimal rendezvous near a point in general keplerian orbit. *Journal of Guidance, Control and Dynamics*, 10(6):567–573, November 1987.

[17] G. Inalhan, M. Tillerson, and J.P. How. Relative dynamics and control of spacecraft formations in eccentric orbits. *Journal of Guidance, Control and Dynamics*, 25(1):48–60, January 2002.

[18] E. Kolemen and N.J. Kasdin. Relative spacecraft motion: A hamiltonian approach to eccentricity perturbations. In *Proceedings of the AAS/AIAA Space Flight Mechanics Meeting*, number AAS-04-294, February 2004. Maui, HI.